

**Patterns and persistence of hydrologic carbon**

B. W. Abbott et al.

This discussion paper is/has been under review for the journal Biogeosciences (BG).  
Please refer to the corresponding final paper in BG if available.

# Patterns and persistence of hydrologic carbon and nutrient export from collapsing upland permafrost

**B. W. Abbott<sup>1,2</sup>, J. B. Jones<sup>1</sup>, S. E. Godsey<sup>3</sup>, J. R. Larouche<sup>4</sup>, and W. B. Bowden<sup>4</sup>**

<sup>1</sup>Department of Biology and Wildlife and Institute of Arctic Biology, University of Alaska Fairbanks, Fairbanks, USA

<sup>2</sup>Université de Rennes 1, OSUR, CNRS, UMR6553 ECOBIO, Rennes, France

<sup>3</sup>Department of Geosciences, Idaho State University, Pocatello, USA

<sup>4</sup>The Rubenstein School of Environment and Natural Resources, University of Vermont, Burlington, USA

Received: 1 January 2015 – Accepted: 12 January 2015 – Published: 2 February 2015

Correspondence to: B. W. Abbott (benabbo@gmail.com)

Published by Copernicus Publications on behalf of the European Geosciences Union.

Title Page

Abstract

Introduction

Conclusions

References

Tables

Figures



Back

Close

Full Screen / Esc

Printer-friendly Version

Interactive Discussion



## Abstract

As high latitudes warm, vast stocks of carbon and nitrogen stored in permafrost will become available for transport to aquatic ecosystems. While there is a growing understanding of the potential effects of permafrost collapse (thermokarst) on aquatic biogeochemical cycles, neither the spatial extent nor temporal duration of these effects are known. To test hypotheses concerning patterns and persistence of elemental export from upland thermokarst, we sampled hydrologic outflow from 83 thermokarst features in various stages of development across the North Slope of Alaska. We hypothesized that an initial pulse of carbon and nutrients would be followed by a period of elemental retention during feature recovery, and that the duration of these stages would depend on feature morphology. Thermokarst caused substantial increases of dissolved organic carbon and other solute concentrations with a particularly large impact on inorganic nitrogen. Magnitude and duration of thermokarst effects on water chemistry differed by feature type and secondarily by landscape age. Most solutes returned to undisturbed concentrations after feature stabilization, but elevated dissolved carbon, inorganic nitrogen, and sulfate concentrations persisted through stabilization for some feature types, suggesting that aquatic disturbance by thermokarst for these solutes is long-lived. Dissolved methane decreased by 90% for most feature types, potentially due to high concentrations of sulfate and inorganic nitrogen. Spatial patterns of carbon and nutrient export from thermokarst suggest that upland thermokarst may be a dominant linkage transferring carbon and nutrients from terrestrial to aquatic ecosystems as the Arctic warms.

## 1 Introduction

Arctic tundra and boreal forest have accumulated a vast pool of organic carbon, twice as large as the atmospheric carbon pool and three times as large as the carbon contained by all living things (Hugelius et al., 2014; Tarnocai et al., 2009). Climate change

BGD

12, 2063–2100, 2015

## Patterns and persistence of hydrologic carbon

B. W. Abbott et al.

Title Page

Abstract

Introduction

Conclusions

References

Tables

Figures



Back

Close

Full Screen / Esc

Printer-friendly Version

Interactive Discussion



## Patterns and persistence of hydrologic carbon

B. W. Abbott et al.

[Title Page](#)

[Abstract](#)

[Introduction](#)

[Conclusions](#)

[References](#)

[Tables](#)

[Figures](#)



[Back](#)

[Close](#)

[Full Screen / Esc](#)

[Printer-friendly Version](#)

[Interactive Discussion](#)



is simultaneously causing widespread permafrost degradation (Slater and Lawrence, 2013) and altering high-latitude hydrology (Peterson et al., 2006; Rawlins et al., 2010), exposing carbon and other elements previously protected in permafrost to transport and processing in Arctic rivers, lakes, and estuaries. Fluxes of dissolved organic carbon (DOC), nutrients, and other ions are changing across the permafrost region and the rate of change is projected to accelerate (Frey and McClelland, 2009; Jones et al., 2005; Laudon et al., 2012; McClelland et al., 2007, 2014; O'Donnell et al., 2012; Petrone et al., 2006; Rawlins et al., 2010; Striegl et al., 2005; Tank et al., 2012). The interaction between changing hydrology and degrading permafrost is one of the key uncertainties in predicting the response of aquatic ecosystems to high-latitude climate change (Abbott et al., 2014a; Koch et al., 2013b; McClelland et al., 2008; Rawlins et al., 2010; Vonk and Gustafsson, 2013).

Permafrost degradation follows two basic trajectories. In permafrost with little ground ice, the soil profile can thaw from the top down without disturbing the surface, gradually exposing organic matter and solutes to hydrologic export (Koch et al., 2013a; Petrone et al., 2006; Striegl et al., 2005). Alternatively, in permafrost where ground ice volume exceeds soil pore space, thaw causes surface subsidence or collapse, termed thermokarst (Kokelj and Jorgenson, 2013). When thermokarst occurs on hillslopes it can abruptly mobilize sediment, organic matter, and solutes from meters below the surface, impacting kilometers of stream reach or entire lakes (Bowden et al., 2008; Kokelj et al., 2005, 2013; Vonk et al., 2012).

The term thermokarst includes a suite of thermo-erosional features with different morphologies determined primarily by ice content, substrate type, landscape position, and slope (Osterkamp et al., 2009). In upland landscapes, the three most common thermokarst morphologies are retrogressive thaw slumps, active-layer detachment slides, and thermo-erosion gullies (Jorgenson and Osterkamp, 2005; Kokelj and Jorgenson, 2013; Krieger, 2012). Thaw slumps often form on lakeshores, have a retreating headwall, and are fueled by a variety of ground ice types. Active-layer detachment slides form when the seasonally thawed surface layer of vegetation and soil slips

downhill over an ice-rich transition zone. Thermo-erosion gullies form due to melting of ice wedges, growing with a generally linear or dendritic pattern, and are often associated with water tracks or headwater streams. These three morphologies currently impact ca. 1.5 % of the landscape in the western foothills of the Brooks Range (Krieger, 2012) and could affect 20–50 % of uplands in the continuous permafrost region by the end of the century based on projected thaw and estimates of ground ice distribution (Slater and Lawrence, 2013; Zhang et al., 2000), though circumarctic prevalence and development of upland thermokarst are poorly constrained (Jorgenson et al., 2006; Lantz and Kokelj, 2008; Yoshikawa et al., 2002).

Upland thermokarst can alter the age and degradability of organic carbon, releasing older particulate organic carbon (Lafreniere and Lamoureux, 2013) and more labile DOC during formation (Abbott et al., 2014b; Cory et al., 2013; Vonk et al., 2013). Mineral soil exposed by thermokarst can increase solutes available for hydrologic transport (Harms et al., 2013; Kokelj and Burn, 2003; Kokelj et al., 2013; Louiseize et al., 2014), but can also adsorb DOC, reducing concentration in feature outflows and receiving waters, resulting in greater water clarity after sediment loading and settling (Kokelj et al., 2005; Thompson et al., 2012). These changes in sediment delivery, light penetration, and nutrients can alter aquatic food webs in receiving ecosystems (Mesquita et al., 2010; Thienpont et al., 2013; Thompson et al., 2012).

Despite a growing understanding of the potential effects of upland thermokarst on aquatic biogeochemical cycles, there is conflicting evidence on the temporal duration of these effects and their overall importance to ecological functioning, precluding conceptualization of patterns of thermokarst impacts and their incorporation into coupled climate models. If thermokarst disturbance is hydrologically connected to aquatic ecosystems, substantial loading of sediment, carbon, and nutrients can occur (Bowden et al., 2008; Kokelj et al., 2005, 2013; Shirokova et al., 2013; Thienpont et al., 2013; Vonk et al., 2013), though not all features connected to surface waters result in enhanced carbon and nutrient export (Thompson et al., 2012). Conversely, if thermokarst is hydrologically isolated from surface waters, such as when failures occur high on hill-

## BGD

12, 2063–2100, 2015

### Patterns and persistence of hydrologic carbon

B. W. Abbott et al.

Title Page

Abstract

Introduction

Conclusions

References

Tables

Figures



Back

Close

Full Screen / Esc

Printer-friendly Version

Interactive Discussion



slopes, even dramatic disturbance can have little or no impact on aquatic chemistry and elemental budgets (Lafreniere and Lamoureux, 2013; Lewis et al., 2012). The duration of carbon and nutrient release, and the persistence of biogeochemical disturbance in affected ecosystems after feature stabilization is largely unknown, with altered surface water chemistry lasting for decades in some cases of nutrient loading or surface disturbance (Kokelj et al., 2005; Thienpont et al., 2013), or fading after less than a year in others (Lafreniere and Lamoureux, 2013).

To address these knowledge gaps, we sampled surface outflow from thermokarst features in various stages of development across a broad portion of the North Slope of Alaska. We focused on two questions. First, how does thermokarst formation alter hydrologic release of carbon and nutrients, and second, can the type and duration of hydrologic release be predicted based on feature morphology or landscape characteristics? We hypothesized that upland thermokarst would initially stimulate nutrient release due to disruption of soil aggregates, accelerated mineralization in impacted soils, decreased plant uptake, and direct release from melting ground-ice. However, following nutrient retention theory (Vitousek and Reiners, 1975), we hypothesized that this pulse of nutrients would be followed by a period of elemental retention due to enhanced nutrient uptake by recovering vegetation and diminished pools of organic matter and nutrients following disturbance. We hypothesized that DOC export would depend on the balance between DOC production from soil disruption and DOC removal via adsorption by exposed mineral soil as well as enhanced processing of DOC within features due to abundant nutrients and biodegradable DOC from permafrost. In regards to feature morphology, we hypothesized that fundamental differences in formation and functioning of slides, gullies, and slumps, such as the amount of organic and mineral soil displaced, type of ground ice, location on the landscape, and duration of disturbance would result in systematic differences in carbon and nutrient release. We predicted that slumps would have the largest and longest impact, slides would have a large but short-lived impact, and gullies would have a muted impact of intermediate duration.

## Patterns and persistence of hydrologic carbon

B. W. Abbott et al.

[Title Page](#)[Abstract](#)[Introduction](#)[Conclusions](#)[References](#)[Tables](#)[Figures](#)[Back](#)[Close](#)[Full Screen / Esc](#)[Printer-friendly Version](#)[Interactive Discussion](#)

## 2 Methods

### 2.1 Study sites

We tested our hypotheses about thermokarst carbon and nutrient export with observations from 83 slides, gullies, and slumps on the North Slope of Alaska (Fig. 1). Features were identified by aerial surveys, satellite imagery, and previous studies (Abbott et al., 2014b; Bowden et al., 2008; Gooseff et al., 2009) and were located in three areas of upland tundra underlain by continuous permafrost in the foothills of the Brooks Range. We collected samples during the growing season (June–August) of 2009–2012 and May of 2011 in the region surrounding the Toolik Field Station, with additional sampling in the Noatak National Preserve near the Kelly River Ranger Station in 2010 and Feniak Lake in 2011.

The Toolik Field Station is located 254 km north of the Arctic Circle and 180 km south of the Arctic Ocean. The mean annual temperature is  $-10^{\circ}\text{C}$  with mean monthly temperatures ranging from  $-25^{\circ}\text{C}$  in January to  $11.5^{\circ}\text{C}$  in July. The region receives 320 mm of precipitation annually with 200 mm falling between June and August (Toolik Environmental Data Center Team, 2014). Feniak Lake is located 360 km west of the Toolik Field Station in the central Brooks Range at the northeast border of the Noatak National Preserve. The average annual temperature is  $-7^{\circ}\text{C}$  (Jorgenson et al., 2008) and average precipitation is 450 mm (WRCC, 2011). The Kelly River Ranger Station is located on the western border of the Noatak National Preserve, 170 km west of Feniak Lake. Average annual temperature is  $-5.4^{\circ}\text{C}$  and the area receives an average of 300 mm of precipitation, a third of which falls during the growing season (Stottlemeyer, 2001).

Vegetation is typical of Arctic tundra across the study region and includes moist acid tundra characterized by the tussock-forming sedge *Eriophorum vaginatum*, moist non-acidic tundra, and shrub tundra (Bhatt et al., 2010; Walker et al., 1998), with isolated stands of white spruce (*Picea glauca*) near the Kelly River Ranger Station (Sullivan and Sveinbjornsson, 2010). All three areas occur in bioclimate subzone E, the warmest re-

BGD

12, 2063–2100, 2015

## Patterns and persistence of hydrologic carbon

B. W. Abbott et al.

Title Page

Abstract

Introduction

Conclusions

References

Tables

Figures



Back

Close

Full Screen / Esc

Printer-friendly Version

Interactive Discussion



gion in the continuous permafrost zone (Walker et al., 2010). The foothills of the Brooks Range have been affected by multiple glaciations starting in the late Tertiary and continuing to 11 ka B.P. (Hamilton, 2003). Repeated rounds of glacial advance and retreat have resulted in a patchwork of glacial till, bedrock, and loess parent materials of various ages (Hamilton, 2010). Time since last glaciation can be associated with ecosystem properties including pH, organic layer depth, nutrient pools, vegetation community, and biogeochemical rates (Epstein et al., 2004; Hobbie et al., 2002; Lee et al., 2011; Walker et al., 1998).

## 2.2 Experimental design and sampling

To test our hypotheses concerning the intensity and duration of thermokarst impacts on aquatic chemistry, we sampled thermokarst features in all stages of development across landscape ages and vegetation types. We collected water from 83 thermokarst outflows and 61 adjacent undisturbed water bodies such as water tracks and first-order streams (22 locations did not have a suitable paired reference site). To quantify the evolution and duration of thermokarst effects through time, we classified features on a 0–3 index following the development of a hypothetical feature from before initiation (0) to after stabilization (3). Development stages were defined as follows: (0) no apparent present or past thermo-degradation, (1) active thermo-degradation (> 25 % of headwall is actively expanding) with completely turbid outflow, (2) moderate thermo-degradation (< 25 % of headwall is expanding) with somewhat turbid outflow, and (3) stabilized or limited thermo-degradation with complete or partial revegetation and clear outflow.

Vegetation class was determined in the field and cross-referenced with published vegetation maps when available (Walker et al., 2005). Glacial geology and surface age were based on recent maps of the study region (Hamilton, 2010, 2003; Kanevskiy et al., 2011). Most site ages ranged from 10–200 ka, though six sites occurred on surfaces unglaciated for more than 1000 ka. We classified sites on surfaces younger than 25 ka as young, and sites over 50 ka as old, corresponding to the split between the Iltkilik I and II advances (Hamilton, 2003).

Title Page

Abstract

Introduction

Conclusions

References

Tables

Figures



Back

Close

Full Screen / Esc

Printer-friendly Version

Interactive Discussion



**Patterns and  
persistence of  
hydrologic carbon**

B. W. Abbott et al.

[Title Page](#)[Abstract](#)[Introduction](#)[Conclusions](#)[References](#)[Tables](#)[Figures](#)[Back](#)[Close](#)[Full Screen / Esc](#)[Printer-friendly Version](#)[Interactive Discussion](#)

Samples for carbon and nutrient analysis were filtered in the field (0.7  $\mu\text{m}$  effective pore size, Advantec GF-75) into 60 mL high density polyethylene (HDPE) bottles, except when excess sediment required settling overnight when samples were filtered within 24 h. After filtration, samples were frozen until analysis. We measured DOC and dissolved inorganic carbon (DIC) with a Shimadzu TOC-5000 connected to an Antek 7050 chemiluminescent detector to quantify total dissolved nitrogen after combustion to  $\text{NO}_x$ . We analyzed major ions ( $\text{NO}_3^-$ ,  $\text{NO}_2^-$ ,  $\text{SO}_4^{2-}$ ,  $\text{Cl}^-$ ,  $\text{NH}_4^+$ ,  $\text{Ca}^{2+}$ ,  $\text{Na}^+$ ,  $\text{Mg}^{2+}$ , and  $\text{K}^+$ ) on a Dionex DX-320 ion chromatograph. We calculated dissolved organic nitrogen (DON) by subtracting dissolved inorganic nitrogen ( $\text{DIN} = \text{NO}_3^- + \text{NH}_4^+ + \text{NO}_2^-$ ) from total dissolved nitrogen, and we calculated the DOC to DON ratio (C : N) of dissolved organic matter, an indicator of organic matter source and degree of prior processing (Amon et al., 2012). To determine the percentage of thermokarst outflow coming from ground ice, we analyzed  $\delta\text{D}$  and  $\delta^{18}\text{O}$  on a Picarro L1102-i via cavity ringdown spectroscopy.

Because lateral fluxes of dissolved gas can constitute a considerable portion of Arctic carbon budgets (Kling et al., 1992; Striegl et al., 2012), we measured dissolved  $\text{CO}_2$ ,  $\text{CH}_4$ , and  $\text{N}_2\text{O}$  in feature outflows and reference water. At each site we collected a 30 mL sample of bubble-free water in a 60 mL gas-tight syringe accompanied by an ambient atmospheric sample in a 15 mL evacuated gas vial. Upon return to the lab or camp we added 30 mL of atmosphere to the syringe and shook vigorously for two minutes to facilitate equilibration of dissolved gases with the introduced headspace, and then injected a sample of the headspace into an evacuated gas vial for storage until analysis. We determined  $\text{CO}_2$ ,  $\text{CH}_4$ , and  $\text{N}_2\text{O}$  concentration of the headspace sample on a Varian 3300 gas chromatograph with a flame ionization detector and methanizer for carbon species and an electron capture detector for  $\text{N}_2\text{O}$ . We calculated the proportion of total gas dissolved in solution and in the headspace using Henry's constants adjusted for extraction temperature (Wilhelm et al., 1977), and subtracted ambient gas introduced during extraction to determine initial concentration. We calculated saturation

tion as the percent of equilibrium water concentration based on atmospheric partial pressure and water temperatures at the time of sampling and extraction.

To determine the direct contribution of carbon and nutrients from ground ice, we sampled exposed headwall ice at 24 sites. We collected ice scrapings into Ziplock™ bags, which we filtered and analyzed after melt as previously described. We compared concentrations of carbon and nutrients in ground ice to feature outflows to determine whether solute concentrations were changing as water flowed through the feature. At these sites we used the difference between the  $\delta^{18}\text{O}$  of ground ice and adjacent reference water to determine the proportion of outflow contributed by ground ice. We calculated the proportion from ground ice with a simple two end-member model:

$$\text{Fraction from ground ice} = (\delta^{18}\text{O}_{\text{out}} - \delta^{18}\text{O}_{\text{sw}}) / (\delta^{18}\text{O}_{\text{ice}} - \delta^{18}\text{O}_{\text{sw}}) \quad (1)$$

where out is feature outflow, sw is undisturbed surface water, and ice is headwall ice.

We measured discharge from 26 thermokarst features using salt-dilution gauging. We logged electrical conductivity with a YSI Professional Plus conductivity meter and added 10–100 g of dissolved NaCl upstream of the probe by 10–20 m, depending on the size of the outflow. Discharge was determined by total dilution of the tracer as it passed by the probe (Wlostowski et al., 2013). We mapped feature perimeters with a commercial-grade, handheld GPS, except for four sites around Toolik, which were mapped by the Toolik Field Station GIS staff with a survey-grade GPS and base station.

### 2.3 Statistical analyses

We used a linear mixed-effects model to test for effects of thermokarst development stage, feature type, vegetation, and landscape age on water chemistry while accounting for spatial and temporal non-independence in the data. For each water chemistry parameter we used a mixed-effects analysis of variance (ANOVA) with development stage crossed with feature type and vegetation and landscape age as fixed effects. We included site as a random effect to pair thermokarst outflows with their adjacent reference water. We visually inspected residual plots for deviations from normality and

## Patterns and persistence of hydrologic carbon

B. W. Abbott et al.

Title Page

Abstract

Introduction

Conclusions

References

Tables

Figures



Back

Close

Full Screen / Esc

Printer-friendly Version

Interactive Discussion



homoscedasticity, and transformed response and predictor variables when necessary. We simplified the full model by automated backwards elimination, using restricted maximum likelihood to evaluate fixed effects and likelihood ratio tests for random effects. To test for differences between groups, we performed post-hoc Tukey honest significant difference tests on the least squares means using Satterthwaite approximation to estimate denominator degrees of freedom. We used Pearson product-moment correlation to test for associations between water chemistry parameters and development stage, which we recoded low to high and treated as a continuous variable of disturbance intensity. A decision criterion of  $\alpha = 0.05$  was used for all tests.

All analyses were performed in R 3.0.2 (R Core Team, 2013) with the lme4 and lmerTest packages (Bates et al., 2013; Kuznetsova et al., 2014). The complete dataset is available through the Advanced Cooperative Arctic Data and Information Service at [www.aoncadis.org/dataset/soil\\_water\\_gas\\_alaskan\\_thermokarst.html](http://www.aoncadis.org/dataset/soil_water_gas_alaskan_thermokarst.html).

### 3 Results

#### 3.1 Thermokarst distribution and characteristics

Feature types were not distributed equally among vegetation classes with most active-layer detachment slides occurring on non-acidic tundra, most thermo-erosion gullies occurring on acidic tundra, and thaw slumps distributed among tundra types (Table 1). Feature types were also unevenly distributed between development stages with over half of slumps classified as stage 1 (very active) compared to approximately 30% of slides and gullies. Over 90% of all features were associated with, or intersected a water body (Table 1). Slides and gullies occurred primarily on or next to water tracks or headwater streams and the majority of thaw slumps were on lakeshores. Slides tended to occur in the highest topographic positions, slumps were distributed across high and low gradient surfaces, and gullies were most common on foot slopes or valley bottoms.

## BGD

12, 2063–2100, 2015

### Patterns and persistence of hydrologic carbon

B. W. Abbott et al.

Title Page

Abstract

Introduction

Conclusions

References

Tables

Figures



Back

Close

Full Screen / Esc

Printer-friendly Version

Interactive Discussion



Discharge from thermokarst features varied widely by feature type and individual features in the study, from no flow at some stabilized slumps and slides to  $9.4 \text{ L s}^{-1}$  at one slide (Table 1). Mean discharge was highest for slides and lowest for slumps. For sites where we estimated the proportion of outflow derived from ground ice, the ice contribution varied from 0–97%. Slumps had the highest average ground ice contribution and slides had the lowest, though these values are not representative of all features, since they are only based on sites with exposed ground ice. Generally sites with high discharge ( $> 2 \text{ L s}^{-1}$ ) had little contribution from ground ice, except several large slumps with very active headwall retreat.

### 3.2 Effects of development stage and morphology on water chemistry

Thermokarst significantly altered concentrations of carbon, nitrogen, and other solutes but the magnitude and duration of these effects differed by feature type (Figs. 2–4). For most parameters, effects were largest at the most active features, with differences tapering off as activity decreased. However, DOC in slide outflows as well as DIC,  $\text{Mg}^{2+}$ ,  $\text{Ca}^+$ , and dissolved  $\text{N}_2\text{O}$  concentrations in gully outflows were highest in stabilized features. Slumps tended to have the largest effect on solute concentrations. For example,  $\text{SO}_4^{2-}$  concentration was 30-fold higher than reference in stage-1 outflows, compared to 3.3- and 1.5-fold higher for gullies and slides, respectively. Gully reference and outflow chemistry was generally distinct from slides and slumps, with higher dissolved gas concentrations and DOC : DON, but lower concentrations of ions and DIC.

Thaw slumps caused the greatest increase in dissolved organic matter concentration, with DOC and DON 2.6- and 4.0-fold greater in stage-1 features, compared with 1.6- and 1.4-fold increases in slides, and 2.2- and 1.6-fold increases in gullies of DOC and DON, respectively (Fig. 2). Thermokarst had a much larger impact on inorganic nitrogen, with mean  $\text{NH}_4^+$  and  $\text{NO}_3^-$  concentrations 9- to 27-fold greater in stage-1 features (Fig. 3). Consequently, the relative proportion of DIN, which made up less than 10% of total nitrogen in reference waters, constituted 26 to 38% of total nitrogen in stage-1 features and 48% of total nitrogen in stage-2 gullies (Fig. 5).  $\text{NH}_4^+$  was the

BGD

12, 2063–2100, 2015

## Patterns and persistence of hydrologic carbon

B. W. Abbott et al.

Title Page

Abstract

Introduction

Conclusions

References

Tables

Figures

⏪

⏩

◀

▶

Back

Close

Full Screen / Esc

Printer-friendly Version

Interactive Discussion



dominant form of DIN for all feature types and development stages except stage-3 (stabilized) slides where  $\text{NO}_3^-$  made up 70 % of DIN. Elevated DIN persisted through stage 2 for slumps and through stabilization for gullies.

Dissolved  $\text{CH}_4$  concentration was 92 and 89 % lower than reference for stage-1 gullies and slumps, respectively (Fig. 2). However, there were no significant differences by development stage for dissolved  $\text{CO}_2$  and dissolved  $\text{N}_2\text{O}$  was only significantly elevated in stabilized gullies. Across all development stages and feature types, 93 and 97 % of all samples were supersaturated with  $\text{CO}_2$  and  $\text{CH}_4$ , respectively, whereas 51 % of samples were supersaturated with  $\text{N}_2\text{O}$ .

### 3.3 Ground-ice, vegetation, and landscape age

Permafrost ice was high in dissolved carbon, nitrogen, and solutes and had a depleted  $\delta^{18}\text{O}$  signature relative to reference waters (Table 3). Average concentrations of DIC,  $\text{NH}_4^+$ , and  $\text{K}^+$  were higher in ground ice than feature outflow, indicating uptake or dilution during transport from the feature headwall to outflow. However, all other solutes, notably DOC,  $\text{NO}_3^-$ , and  $\text{SO}_4^{2-}$ , were higher in outflows than in ground ice, indicating net production or contribution from soils or more concentrated flowpaths during transit.

Landscape age modulated the effect of upland thermokarst on water chemistry, with much larger differences between impacted and undisturbed concentrations of DOC,  $\text{NH}_4^+$ ,  $\text{Cl}^-$  and  $\text{SO}_4^{2-}$  at sites occurring on surfaces older than 50 ka (Fig. 6). Vegetation had a smaller effect on fewer parameters with only DOC,  $\text{Ca}^+$ , and  $\text{Cl}^-$  differing significantly by vegetation community independent of development stage, feature type, and landscape age, with different patterns between vegetation communities for each solute (Fig. 7).

BGD

12, 2063–2100, 2015

## Patterns and persistence of hydrologic carbon

B. W. Abbott et al.

Title Page

Abstract

Introduction

Conclusions

References

Tables

Figures



Back

Close

Full Screen / Esc

Printer-friendly Version

Interactive Discussion



## 4 Discussion

There is conflicting evidence of the impacts of upland thermokarst on concentrations and fluxes of DOC, nutrients, and other solutes (Bowden et al., 2008; Thompson et al., 2012), as well as the intensity and duration of these effects (Kokelj et al., 2005; Lafreniere and Lamoureux, 2013; Thienpont et al., 2013). Our spatially extensive sampling of active and stabilized features revealed that upland thermokarst consistently increases DOC and other solute concentrations with a particularly large effect on inorganic nitrogen. Magnitude and duration of thermokarst effects on water chemistry differed by feature type and secondarily by landscape age. Most solutes returned to undisturbed concentrations after feature stabilization, but elevated inorganic nitrogen and several other parameters persisted in gully and slump outflows, suggesting these feature types could have long-lasting impacts on aquatic nutrient dynamics.

### 4.1 Patterns of carbon and nitrogen release from upland thermokarst

We hypothesized that thermokarst would increase or decrease DOC concentration in surface waters depending on the balance of DOC production and removal processes active during feature formation. Despite large organic layer losses and abundant exposed mineral soil (Pizano et al., 2014), upland thermokarst significantly increased average DOC concentration and yield for all feature types. Additionally, DOC from active thermokarst features is three to four times more bio- and photo-degradable than active-layer-derived DOC (Abbott et al., 2014b; Cory et al., 2013) changing the implications of this release at different spatial scales. Thermokarst DOC is likely to be mineralized rapidly in receiving soils, streams, and lakes, accelerating transfer of permafrost carbon to the atmosphere (Vonk et al., 2013) but reducing the impact of this disturbance on estuaries of the Arctic Ocean (McClelland et al., 2012; Striegl et al., 2005).

Upland thermokarst had a relatively larger effect on aquatic nitrogen than carbon concentrations, reducing the C : N ratio of dissolved organic matter and causing substantial and long-lasting release of inorganic nitrogen. Phosphorus, not nitrogen, is typ-

BGD

12, 2063–2100, 2015

## Patterns and persistence of hydrologic carbon

B. W. Abbott et al.

Title Page

Abstract

Introduction

Conclusions

References

Tables

Figures



Back

Close

Full Screen / Esc

Printer-friendly Version

Interactive Discussion



## Patterns and persistence of hydrologic carbon

B. W. Abbott et al.

[Title Page](#)

[Abstract](#)

[Introduction](#)

[Conclusions](#)

[References](#)

[Tables](#)

[Figures](#)



[Back](#)

[Close](#)

[Full Screen / Esc](#)

[Printer-friendly Version](#)

[Interactive Discussion](#)



ically the most limiting nutrient in Arctic freshwater systems (O'Brien et al., 2005; Slavik et al., 2004), however, nitrogen and silica limit productivity in Arctic estuaries and the Arctic Ocean (McClelland et al., 2012; Vancoppenolle et al., 2013). If thermokarst nitrogen release is accompanied by bioavailable phosphorus, more nitrogen will be retained in inland aquatic ecosystems, whereas if thermokarst outflows have relatively little phosphorus, a larger proportion of liberated nitrogen will reach the ocean. Thermokarst can increase phosphorus loading (Bowden et al., 2008; Hobbie et al., 1999), but the relative impact of upland thermokarst on nutrient stoichiometry remains an important unknown.

Along with changes in solute concentrations and characteristics, upland thermokarst may affect the seasonality of solute flux. For most aquatic ecosystems in the Arctic, the majority of annual carbon and nutrient load occurs during snowmelt or early spring (Holmes et al., 2012). However, carbon and nutrient release from upland thermokarst is determined by feature activity, which depends primarily on air temperature and net radiation, peaking in mid to late summer (Kokelj and Jorgenson, 2013; Lantuit and Pollard, 2005; Lantz and Kokelj, 2008). Late-season delivery of carbon and nitrogen would have a larger relative impact on surface water concentrations, further modifying functioning of Arctic rivers and lakes. This shift could also affect Arctic estuaries, where nutrients and carbon are taken up quickly during open-water season but transported to the Arctic Ocean during ice cover (Townsend-Small et al., 2011).

Feature morphology strongly influenced magnitude and duration of thermokarst effects on water chemistry, with slides having a smaller and shorter impact than gullies or slumps. This could be due to differences in feature depth and duration of feature growth. In permafrost soil, leachable solutes are typically highest below the transition layer at the top of the permafrost table (Keller et al., 2007; Kokelj and Burn, 2003; Malone et al., 2013) and the age and characteristics of soil carbon differ strongly with depth (Guo et al., 2007; Neff et al., 2006; Nowinski et al., 2010; Schuur et al., 2009). Shallow slides are less likely to expose deeper, solute-rich soils to hydrologic export than slumps and gullies, which cut meters into permafrost. However, slides caused a sim-



formation.  $\text{SO}_4^{2-}$  is an energetically favorable electron acceptor compared to the low molecular weight organic compounds or  $\text{CO}_2$  used by methanogens (Dar et al., 2008), and sulfate-reducing bacteria can inhibit methane production through competition for molecular substrates (Muyzer and Stams, 2008).  $\text{SO}_4^{2-}$  concentration was negatively associated with dissolved  $\text{CH}_4$  across site types and development stages, further supporting this hypothesis. However,  $\text{SO}_4^{2-}$  release does not explain decreased dissolved  $\text{CH}_4$  in gully outflows since we observed no change in gully  $\text{SO}_4^{2-}$ . One possibility is that high inorganic nitrogen concentration is stimulating  $\text{CH}_4$  consumption in gully and slump outflows. While elevated DIN can suppress high-affinity methanotrophs responsible for  $\text{CH}_4$  oxidation in low- $\text{CH}_4$  environments, DIN can stimulate consumption by low-affinity methanotrophs that dominate consumption in high  $\text{CH}_4$  environments and are commonly nitrogen-limited (Bodelier and Laanbroek, 2004). This would explain the large  $\text{CH}_4$  decrease in gully outflows where  $\text{CH}_4$  concentration was high, and the lack of response in slide outflows where  $\text{CH}_4$  was 10-fold lower despite similar changes in DIN concentration.

Similar concentrations of  $\text{SO}_4^{2-}$  have been observed in outflows of thaw slumps in the Mackenzie delta (Kokelj et al., 2005; Malone et al., 2013) and there is evidence of enhanced sulfur availability in lakes throughout the Arctic (Drevnick et al., 2010). The widespread release of  $\text{SO}_4^{2-}$  from upland thermokarst may have important implications for carbon cycling as the permafrost region thaws. Increases in freshwater  $\text{SO}_4^{2-}$  could accelerate anaerobic decomposition of organic carbon liberated from permafrost (Eisele et al., 2001) and suppress  $\text{CH}_4$  production after permafrost thaw, modulating one of the key feedbacks from the permafrost system on global climate (Walter et al., 2006).

### 4.3 Where is thermokarst nitrogen coming from?

Though primary production in high-latitude terrestrial ecosystems tends to be limited by nitrogen, suggesting that bioavailable forms of nitrogen should be retained (Vitousek and Reiners, 1975), there are numerous reports of inorganic nitrogen loss from land-

## Patterns and persistence of hydrologic carbon

B. W. Abbott et al.

Title Page

Abstract

Introduction

Conclusions

References

Tables

Figures



Back

Close

Full Screen / Esc

Printer-friendly Version

Interactive Discussion



scapes affected by permafrost degradation (Jones et al., 2005; Mack et al., 2004; McClelland et al., 2007). Contrary to our hypothesis that high demand for nutrients by re-establishing plants would decrease nutrient concentrations in thermokarst outflows during recovery,  $\text{NH}_4^+$  concentration was elevated in stabilized gullies and in no case was DIN significantly lower in recovering features than in undisturbed tundra. This suggests that either nitrogen is not limiting plant growth during revegetation or pathways of nitrogen loss bypass locations of high uptake (e.g. preferential flowpaths below plant rooting zones).

Microenvironments in thermokarst can favor deciduous shrub establishment including nitrogen-fixing species (Lantz et al., 2009), a potential source for thermokarst nitrogen. However, even in the absence of nitrogen-fixing species, surface soils in recovering thermokarst features re-accumulate nitrogen rapidly (Pizano et al., 2014). Upland thermokarst can warm wintertime soil temperature by  $6^\circ\text{C}$  due to conductive heat flux to soils during summer and added insulation in winter from deeper snow (Burn, 2000). If nitrogen mineralization continues through the fall and winter in thawed soils beneath thermokarst scars, hydrologic activity in the spring or deep shrub roots could transport inorganic nitrogen to the surface, fueling productivity and hydrologic export. The isotopic signature of  $\text{NO}_3^-$  draining a high Arctic catchment impacted by upland thermokarst suggests DIN from thermokarst is derived from the heterotrophic decomposition of organic matter found in the mineral soil (Louiseize et al., 2014), supporting this hypothesis. Additionally or alternatively, a portion of inorganic nitrogen in upland thermokarst outflow may come from mineralization of labile dissolved organic matter in the water column or soil solution. This would explain the strong correlation between DIN concentration and DOC biodegradability observed in several Arctic and boreal ecosystems (Abbott et al., 2014b; Balcarczyk et al., 2009; Wickland et al., 2012).

#### 4.4 Shifts in landscape-scale water chemistry

As high latitudes warm, ecosystems are experiencing widespread shifts in aquatic chemistry including an increase in DOC flux in areas with peat and thick organic soil

**BGD**

12, 2063–2100, 2015

### Patterns and persistence of hydrologic carbon

B. W. Abbott et al.

Title Page

Abstract

Introduction

Conclusions

References

Tables

Figures



Back

Close

Full Screen / Esc

Printer-friendly Version

Interactive Discussion



## Patterns and persistence of hydrologic carbon

B. W. Abbott et al.

[Title Page](#)

[Abstract](#)

[Introduction](#)

[Conclusions](#)

[References](#)

[Tables](#)

[Figures](#)



[Back](#)

[Close](#)

[Full Screen / Esc](#)

[Printer-friendly Version](#)

[Interactive Discussion](#)



(Frey and McClelland, 2009), a decrease in DOC where organic soil is shallow (McClelland et al., 2007; Petrone et al., 2006; Striegl et al., 2005), increases in major ion concentrations (Frey and McClelland, 2009; Giesler et al., 2014; Keller et al., 2010), and increased inorganic nutrient flux (Jones et al., 2005; McClelland et al., 2007; Petrone et al., 2006). These changes in catchment-scale solute fluxes have primarily been attributed to mechanisms associated with gradual thaw such as deepening of surface flowpaths and changes in residence time. However, thermokarst may also be contributing to these shifts in catchment-scale chemistry (Frey and McClelland, 2009). The chemical signature of dissolved organic matter from thermokarst closely matches biodegradable DOC recently detected in boreal streams and rivers (Abbott et al., 2014b; Balcarczyk et al., 2009; Wickland et al., 2012) and increases of DIN and solutes from thermokarst match circumpolar changes attributed to a shift towards greater ground-water inputs (Frey and McClelland, 2009; Frey et al., 2007).

Currently a scarcity of observations of the spatial extent and distribution of upland thermokarst features and the annual elemental yields for different feature and landscape types limits our ability to evaluate the relative importance of gradual thaw and thermokarst in determining the evolution of high-latitude biogeochemistry.

## 5 Conclusions

Upland thermokarst across the foothills of the Brooks Range caused substantial increases of inorganic nitrogen, DOC, and other solute concentrations. Thaw slumps and thermo-erosion gullies had larger impacts on solute concentrations and are likely more important than slides to surface water chemistry because they can remain active for multiple years. The delivery of labile carbon and nutrients such as  $\text{SO}_4^{2-}$  and inorganic nitrogen to downstream or downslope ecosystems could have important consequences for offsite carbon cycling, accelerating decomposition of organic matter in anoxic environments and priming the decomposition of recalcitrant organic matter. The fact that individual features can impact entire lakes or river reaches over multiple years

in combination with the large portion of the landscape underlain by ice-rich permafrost suggest that upland thermokarst may be the dominant disturbance affecting aquatic ecosystems as the Arctic warms.

*Author contributions.* B. W. Abbott and J. B. Jones designed the experiment and worked closely on the manuscript written by B. W. Abbott. B. W. Abbott, S. E. Godsey, and J. R. Larouche carried out sample collection, preparation, and analysis. All authors helped refine the experimental design and provided input on the manuscript.

*Acknowledgements.* This work was supported by the National Science Foundation ARCSS program (OPP-0806465 and OPP-0806394). We thank the many individuals and organizations that assisted with this study. T. Chapin, T. Schuur, S. Bret-Harte, and B. Risser gave valuable input on the manuscript. A. Olsson, L. Koenig, and P. Tobin, assisted with lab and fieldwork. Toolik Field Station and CH2M Hill Polar Services provided logistic support. The National Park Service and Bureau of Land Management facilitated research permits. Dedicated to the late A. Bali.

## References

- Abbott, B. W.: Permafrost in a warmer world: net ecosystem carbon imbalance, Ph.D. thesis, Biology and Wildlife, University of Alaska Fairbanks, 331 pp., 2014.
- Abbott, B. W., Jones, J. B., Schuur, E. A. G., Chapin III, F. S., Bowden, W. B., Bret-Harte, M. S., Epstein, H. E., Flannigan, M. D., Harms, T. K., Hollingsworth, T. N., Mack, M. C., McGuire, A. D., Natali, S. M., Rocha, A. V., Tank, S. E., Turetsky, M. R., Vonk, J. E., Wickland, K. P., and Permafrost Carbon Network: Can increased biomass offset carbon release from soils, streams, and wildfire across the permafrost region? An expert elicitation, Nature Climate Change, submitted, 2014a.
- Abbott, B. W., Larouche, J. R., Jones, J. B., Bowden, W. B., and Balsler, A. W.: Elevated dissolved organic carbon biodegradability from thawing and collapsing permafrost, J. Geophys. Res.-Biogeo., 119, 2049–2063, doi:10.1002/2014JG002678, 2014b.
- Amon, R. M. W., Rinehart, A. J., Duan, S., Louchouart, P., Prokushkin, A., Guggenberger, G., Bauch, D., Stedmon, C., Raymond, P. A., Holmes, R. M., McClelland, J. W., Peterson, B. J.,

BGD

12, 2063–2100, 2015

## Patterns and persistence of hydrologic carbon

B. W. Abbott et al.

Title Page

Abstract

Introduction

Conclusions

References

Tables

Figures



Back

Close

Full Screen / Esc

Printer-friendly Version

Interactive Discussion



## Patterns and persistence of hydrologic carbon

B. W. Abbott et al.

Title Page

Abstract

Introduction

Conclusions

References

Tables

Figures



Back

Close

Full Screen / Esc

Printer-friendly Version

Interactive Discussion



Walker, S. A., and Zhulidov, A. V.: Dissolved organic matter sources in large Arctic rivers, *Geochim. Cosmochim. Ac.*, 94, 217–237, 2012.

Balcarczyk, K. L., Jones, J. B., Jaffe, R., and Maie, N.: Stream dissolved organic matter bioavailability and composition in watersheds underlain with discontinuous permafrost, *Biogeochemistry*, 94, 255–270, 2009.

Bates, D., Maechler, M., Bolker, B., and Walker, S.: lme4: Linear mixed-effects models using Eigen and S4, R package version 1.0–5, available at: <http://CRAN.R-project.org/package=lme4> (last access: 24 July 2014), 2013.

Bhatt, U. S., Walker, D. A., Reynolds, M. K., Comiso, J. C., Epstein, H. E., Jia, G. S., Gens, R., Pinzon, J. E., Tucker, C. J., Tweedie, C. E., and Webber, P. J.: Circumpolar Arctic tundra vegetation change is linked to sea ice decline, *Earth Interact.*, 14, 1–20, 2010.

Bodelier, P. L. E. and Laanbroek, H. J.: Nitrogen as a regulatory factor of methane oxidation in soils and sediments, *FEMS Microbiol. Ecol.*, 47, 265–277, 2004.

Bowden, W. B., Gooseff, M. N., Balsler, A., Green, A., Peterson, B. J., and Bradford, J.: Sediment and nutrient delivery from thermokarst features in the foothills of the North Slope, Alaska: potential impacts on headwater stream ecosystems, *J. Geophys. Res.-Biogeo.*, 113, G02026, 1–12, 2008.

Burn, C. R.: The thermal regime of a retrogressive thaw slump near Mayo, Yukon Territory, *Can. J. Earth Sci.*, 37, 967–981, 2000.

Cory, R. M., Crump, B. C., Dobkowski, J. A., and Kling, G. W.: Surface exposure to sunlight stimulates CO<sub>2</sub> release from permafrost soil carbon in the Arctic, *P. Natl. Acad. Sci. USA*, 110, 3429–3434, 2013.

Dar, S. A., Kleerebezem, R., Stams, A. J. M., Kuenen, J. G., and Muyzer, G.: Competition and coexistence of sulfate-reducing bacteria, acetogens and methanogens in a lab-scale anaerobic bioreactor as affected by changing substrate to sulfate ratio, *Appl. Microbiol. Biot.*, 78, 1045–1055, 2008.

Drevnick, P. E., Muir, D. C. G., Lamborg, C. H., Horgan, M. J., Canfield, D. E., Boyle, J. F., and Rose, N. L.: Increased accumulation of sulfur in lake sediments of the High Arctic, *Environ. Sci. Technol.*, 44, 8415–8421, 2010.

Einsele, G., Yan, J. P., and Hinderer, M.: Atmospheric carbon burial in modern lake basins and its significance for the global carbon budget, *Global Planet. Change*, 30, 167–195, 2001.

## BGD

12, 2063–2100, 2015

**Patterns and  
persistence of  
hydrologic carbon**

B. W. Abbott et al.

[Title Page](#)[Abstract](#)[Introduction](#)[Conclusions](#)[References](#)[Tables](#)[Figures](#)[Back](#)[Close](#)[Full Screen / Esc](#)[Printer-friendly Version](#)[Interactive Discussion](#)

Epstein, H. E., Beringer, J., Gould, W. A., Lloyd, A. H., Thompson, C. D., Chapin, F. S., Michaelson, G. J., Ping, C. L., Rupp, T. S., and Walker, D. A.: The nature of spatial transitions in the Arctic, *J. Biogeogr.*, 31, 1917–1933, 2004.

Frey, K. E. and McClelland, J. W.: Impacts of permafrost degradation on arctic river biogeochemistry, *Hydrol. Process.*, 23, 169–182, 2009.

Frey, K. E., McClelland, J. W., Holmes, R. M., and Smith, L. C.: Impacts of climate warming and permafrost thaw on the riverine transport of nitrogen and phosphorus to the Kara Sea, *J. Geophys. Res.-Biogeo.*, 112, 1–10, 2007.

Giesler, R., Lyon, S. W., Mörth, C.-M., Karlsson, J., Karlsson, E. M., Jantze, E. J., Destouni, G., and Humborg, C.: Catchment-scale dissolved carbon concentrations and export estimates across six subarctic streams in northern Sweden, *Biogeosciences*, 11, 525–537, doi:10.5194/bg-11-525-2014, 2014.

Godin, E. and Fortier, D.: Geomorphology of a thermo-erosion gully, Bylot Island, Nunavut, Canada, *Can. J. Earth Sci.*, 49, 979–986, 2012.

Gooseff, M. N., Balser, A., Bowden, W. B., and Jones, J. B.: Effects of Hillslope Thermokarst in Northern Alaska, *Eos, Transactions American Geophysical Union*, 90, 29–30, 2009.

Guo, L. D., Ping, C. L., and Macdonald, R. W.: Mobilization pathways of organic carbon from permafrost to arctic rivers in a changing climate, *Geophys. Res. Lett.*, 34, 1–5, 2007.

Hamilton, T. D.: Surficial Geology of the Dalton Highway (Itkillik-Sagavanirktok Rivers) Area, Southern Arctic foothills, Alaska Division of Geological & Geophysical Surveys, Alaska, Fairbanks, Alaska, 2003.

Hamilton, T. D.: Surficial Geologic Map of the Noatak National Preserve, Alaska, U.S. Geological Survey Scientific Investigations Map 3036, Fairbanks, Alaska, 2010.

Harms, T., Abbott, B., and Jones, J.: Thermo-erosion gullies increase nitrogen available for hydrologic export, *Biogeochemistry*, 117, 1–13, doi:10.1007/s10533-013-9862-0, 2013.

Hobbie, J. E., Peterson, B. J., Bettez, N., Deegan, L., O'Brien, W. J., Kling, G. W., Kipphut, G. W., Bowden, W. B., and Hershey, A. E.: Impact of global change on the biogeochemistry and ecology of an Arctic freshwater system, *Polar Res.*, 18, 207–214, 1999.

Hobbie, S. E., Miley, T. A., and Weiss, M. S.: Carbon and nitrogen cycling in soils from acidic and nonacidic tundra with different glacial histories in Northern Alaska, *Ecosystems*, 5, 761–774, 2002.

Holmes, R. M., McClelland, J. W., Peterson, B. J., Tank, S. E., Bulygina, E., Eglinton, T. I., Gordeev, V. V., Gurtovaya, T. Y., Raymond, P. A., Repeta, D. J., Staples, R., Striegl, R. G.,

## Patterns and persistence of hydrologic carbon

B. W. Abbott et al.

[Title Page](#)

[Abstract](#)

[Introduction](#)

[Conclusions](#)

[References](#)

[Tables](#)

[Figures](#)



[Back](#)

[Close](#)

[Full Screen / Esc](#)

[Printer-friendly Version](#)

[Interactive Discussion](#)



Zhulidov, A. V., and Zimov, S. A.: Seasonal and annual fluxes of nutrients and organic matter from large rivers to the Arctic Ocean and surrounding seas, *Estuar. Coast.*, 35, 369–382, 2012.

Hugelius, G., Strauss, J., Zubrzycki, S., Harden, J. W., Schuur, E. A. G., Ping, C.-L., Schirmer, L., Grosse, G., Michaelson, G. J., Koven, C. D., O'Donnell, J. A., Elberling, B., Mishra, U., Camill, P., Yu, Z., Palmtag, J., and Kuhry, P.: Estimated stocks of circumpolar permafrost carbon with quantified uncertainty ranges and identified data gaps, *Biogeosciences*, 11, 6573–6593, doi:10.5194/bg-11-6573-2014, 2014.

Jones, J. B., Petrone, K. C., Finlay, J. C., Hinzman, L. D., and Bolton, W. R.: Nitrogen loss from watersheds of interior Alaska underlain with discontinuous permafrost, *Geophys. Res. Lett.*, 32, 1–4, 2005.

Jorgenson, M. T. and Osterkamp, T. E.: Response of boreal ecosystems to varying modes of permafrost degradation, *Can. J. Forest Res.*, 35, 2100–2111, 2005.

Jorgenson, M. T., Shur, Y. L., and Pullman, E. R.: Abrupt increase in permafrost degradation in Arctic Alaska, *Geophys. Res. Lett.*, 33, 1–4, 2006.

Jorgenson, M. T., Shur, Y. L., and Osterkamp, T. E.: Thermokarst in Alaska, in: Ninth International Conference On Permafrost, University of Alaska Fairbanks, 29 June–3 July, Fairbanks, Alaska, 117–124, 2008.

Kanevskiy, M., Shur, Y., Fortier, D., Jorgenson, M. T., and Stephani, E.: Cryostratigraphy of late Pleistocene syngenetic permafrost (yedoma) in northern Alaska, Itkillik River exposure, *Quaternary Res.*, 75, 584–596, 2011.

Keller, K., Blum, J. D., and Kling, G. W.: Geochemistry of soils and streams on surfaces of varying ages in Arctic Alaska, *Arct. Antarct. Alp. Res.*, 39, 84–98, 2007.

Keller, K., Blum, J. D., and Kling, G. W.: Stream geochemistry as an indicator of increasing permafrost thaw depth in an arctic watershed, *Chem. Geol.*, 273, 76–81, 2010.

Kling, G. W., Kipphut, G. W., and Miller, M. C.: The flux of CO<sub>2</sub> and CH<sub>4</sub> from lakes and rivers in Arctic Alaska, *Hydrobiologia*, 240, 23–36, 1992.

Koch, J. C., Ewing, S. A., Striegl, R., and McKnight, D. M.: Rapid runoff via shallow throughflow and deeper preferential flow in a boreal catchment underlain by frozen silt (Alaska, USA), *Hydrogeol. J.*, 21, 93–106, 2013a.

Koch, J. C., Runkel, R. L., Striegl, R., and McKnight, D. M.: Hydrologic controls on the transport and cycling of carbon and nitrogen in a boreal catchment underlain by continuous permafrost, *J. Geophys. Res.-Biogeol.*, 118, 698–712, 2013b.

## Patterns and persistence of hydrologic carbon

B. W. Abbott et al.

Title Page

Abstract

Introduction

Conclusions

References

Tables

Figures



Back

Close

Full Screen / Esc

Printer-friendly Version

Interactive Discussion



- Kokelj, S. V. and Burn, C. R.: Ground ice and soluble cations in near-surface permafrost, Inuvik, Northwest Territories, Canada, *Permafrost Periglac.*, 14, 275–289, 2003.
- Kokelj, S. V. and Jorgenson, M. T.: Advances in Thermokarst Research, *Permafrost Periglac.*, 24, 108–119, 2013.
- 5 Kokelj, S. V., Jenkins, R. E., Milburn, D., Burn, C. R., and Snow, N.: The influence of thermokarst disturbance on the water quality of small upland lakes, Mackenzie Delta Region, Northwest Territories, Canada, *Permafrost Periglac.*, 16, 343–353, 2005.
- Kokelj, S. V., Lantz, T. C., Kanigan, J., Smith, S. L., and Coutts, R.: Origin and polycyclic behaviour of Tundra Thaw Slumps, Mackenzie Delta Region, Northwest Territories, Canada, *Permafrost Periglac.*, 20, 173–184, 2009.
- 10 Kokelj, S. V., Lacelle, D., Lantz, T. C., Tunnicliffe, J., Malone, L., Clark, I. D., and Chin, K. S.: Thawing of massive ground ice in mega slumps drives increases in stream sediment and solute flux across a range of watershed scales, *J. Geophys. Res.-Earth*, 118, 681–692, 2013.
- Krieger, K. C.: The Topographic Form and Evolution of Thermal Erosion Features: a First Analysis Using Airborne and Ground-Based LiDAR in Arctic Alaska, M.S. thesis, Geosciences, Idaho State University, Pocatello, Idaho, 98 pp., 2012.
- 15 Kuznetsova, A., Brockhoff, P. B., and Christensen, R. H. B.: lmerTest: tests for random and fixed effects for linear mixed effect models (lmer objects of lme4 package). R package version 2.0–6, available at: <http://CRAN.R-project.org/package=lmerTest> (last access: 24 July 2014), 2014.
- 20 Lafreniere, M. J. and Lamoureux, S. F.: Thermal perturbation and rainfall runoff have greater impact on seasonal solute loads than physical disturbance of the active layer, *Permafrost Periglac.*, 24, 241–251, 2013.
- Lantuit, H. and Pollard, W. H.: Temporal stereophotogrammetric analysis of retrogressive thaw slumps on Herschel Island, Yukon Territory, *Nat. Hazards Earth Syst. Sci.*, 5, 413–423, doi:10.5194/nhess-5-413-2005, 2005.
- 25 Lantz, T. C. and Kokelj, S. V.: Increasing rates of retrogressive thaw slump activity in the Mackenzie Delta region, NWT, Canada, *Geophys. Res. Lett.*, 35, 1–5, 2008.
- Lantz, T. C., Kokelj, S. V., Gergel, S. E., and Henryz, G. H. R.: Relative impacts of disturbance and temperature: persistent changes in microenvironment and vegetation in retrogressive thaw slumps, *Global Change Biol.*, 15, 1664–1675, 2009.
- 30 Laudon, H., Buttle, J., Carey, S. K., McDonnell, J., McGuire, K., Seibert, J., Shanley, J., Soulsby, C., and Tetzlaff, D.: Cross-regional prediction of long-term trajectory

## Patterns and persistence of hydrologic carbon

B. W. Abbott et al.

[Title Page](#)

[Abstract](#)

[Introduction](#)

[Conclusions](#)

[References](#)

[Tables](#)

[Figures](#)



[Back](#)

[Close](#)

[Full Screen / Esc](#)

[Printer-friendly Version](#)

[Interactive Discussion](#)



of stream water DOC response to climate change, *Geophys. Res. Lett.*, 39, L18404, doi:10.1029/2012GL053033, 2012.

Lee, H., Schuur, E. G., Vogel, J. G., Lavoie, M., Bhadra, D., and Staudhammer, C. L.: A spatially explicit analysis to extrapolate carbon fluxes in upland tundra where permafrost is thawing, *Global Change Biol.*, 17, 1379–1393, 2011.

Lewis, T., Lafreniere, M. J., and Lamoureaux, S. F.: Hydrochemical and sedimentary responses of paired High Arctic watersheds to unusual climate and permafrost disturbance, Cape Bounty, Melville Island, Canada, *Hydrol. Process.*, 26, 2003–2018, 2012.

Lewkowicz, A. G.: Nature and importance of thermokarst processes, Sand Hills Moraine, Banks Island, Canada *Geogr. Ann. A*, 69, 321–327, 1987.

Lewkowicz, A. G.: Dynamics of active-layer detachment failures, Fosheim Peninsula, Ellesmere Island, Nunavut, Canada, *Permafrost Periglac.*, 18, 89–103, 2007.

Louiseize, N., Lafrenière, M., and Hastings, M.: Stable isotopic evidence of enhanced export of microbially derived NO<sub>3</sub>- following active layer slope disturbance in the Canadian High Arctic, *Biogeochemistry*, 121, 1–16, doi:10.1007/s10533-014-0023-x, 2014.

Mack, M. C., Schuur, E. A. G., Bret-Harte, M. S., Shaver, G. R., and Chapin, F. S.: Ecosystem carbon storage in arctic tundra reduced by long-term nutrient fertilization, *Nature*, 431, 440–443, 2004.

Malone, L., Lacelle, D., Kokelj, S., and Clark, I. D.: Impacts of hillslope thaw slumps on the geochemistry of permafrost catchments (Stony Creek watershed, NWT, Canada), *Chem. Geol.*, 356, 38–49, 2013.

McClelland, J. W., Holmes, R. M., Dunton, K. H., and Macdonald, R. W.: The Arctic ocean estuary, *Estuar. Coast.*, 35, 353–368, 2012.

McClelland, J. W., Stieglitz, M., Pan, F., Holmes, R. M., and Peterson, B. J.: Recent changes in nitrate and dissolved organic carbon export from the upper Kuparuk River, North Slope, Alaska, *J. Geophys. Res.-Biogeo.*, 112, 1–13, 2007.

McClelland, J. W., Holmes, R. M., Peterson, B. J., Amon, R., Brabets, T., Cooper, L., Gibson, J., Gordeev, V. V., Guay, C., Milburn, D., Staples, R., Raymond, P. A., Shiklomanov, I., Striegl, R., Zhulidov, A., Gurtovaya, T., and Zimov, S.: Development of a Pan-Arctic Database for River Chemistry, *Eos, Transactions American Geophysical Union*, 89, 217–218, 2008.

McClelland, J. W., Townsend-Small, A., Holmes, R. M., Pan, F., Stieglitz, M., Khosh, M., and Peterson, B. J.: River export of nutrients and organic matter from the North Slope of Alaska to the Beaufort Sea, *Water Resour. Res.*, 50, 1823–1839, 2014.

## Patterns and persistence of hydrologic carbon

B. W. Abbott et al.

Title Page

Abstract

Introduction

Conclusions

References

Tables

Figures



Back

Close

Full Screen / Esc

Printer-friendly Version

Interactive Discussion



Mesquita, P. S., Wrona, F. J., and Prowse, T. D.: Effects of retrogressive permafrost thaw slumping on sediment chemistry and submerged macrophytes in Arctic tundra lakes, *Freshwater Biol.*, 55, 2347–2358, 2010.

Muyzer, G. and Stams, A. J. M.: The ecology and biotechnology of sulphate-reducing bacteria, *Nat. Rev. Microbiol.*, 6, 441–454, 2008.

Neff, J. C., Finlay, J. C., Zimov, S. A., Davydov, S. P., Carrasco, J. J., Schuur, E. A. G., and Davydova, A. I.: Seasonal changes in the age and structure of dissolved organic carbon in Siberian rivers and streams, *Geophys. Res. Lett.*, 33, 1–5, 2006.

Nowinski, N. S., Taneva, L., Trumbore, S. E., and Welker, J. M.: Decomposition of old organic matter as a result of deeper active layers in a snow depth manipulation experiment, *Oecologia*, 163, 785–792, 2010.

O'Brien, W. J., Barfield, M., Bettez, N., Hershey, A. E., Hobbie, J. E., Kipphut, G., Kling, G., and Miller, M. C.: Long-term response and recovery to nutrient addition of a partitioned arctic lake, *Freshwater Biol.*, 50, 731–741, 2005.

O'Donnell, J. A., Jorgenson, M. T., Harden, J. W., McGuire, A. D., Kanevskiy, M. Z., and Wickland, K. P.: The effects of permafrost thaw on soil hydrologic, thermal, and carbon dynamics in an Alaskan peatland, *Ecosystems*, 15, 213–229, 2012.

Osterkamp, T. E., Jorgenson, M. T., Schuur, E. A. G., Shur, Y. L., Kanevskiy, M. Z., Vogel, J. G., and Tumskey, V. E.: Physical and ecological changes associated with warming permafrost and thermokarst in interior Alaska, *Permafrost Periglac.*, 20, 235–256, 2009.

Peterson, B. J., McClelland, J., Curry, R., Holmes, R. M., Walsh, J. E., and Aagaard, K.: Trajectory shifts in the Arctic and subarctic freshwater cycle, *Science*, 313, 1061–1066, 2006.

Petrone, K. C., Jones, J. B., Hinzman, L. D., and Boone, R. D.: Seasonal export of carbon, nitrogen, and major solutes from Alaskan catchments with discontinuous permafrost, *J. Geophys. Res.-Biogeo.*, 111, 1–13, 2006.

Pizano, C., Barón, A. F., Schuur, E. A. G., Crummer, K. G., and Mack, M. C.: Effects of thermoerosional disturbance on surface soil carbon and nitrogen dynamics in upland arctic tundra, *Environ. Res. Lett.*, 9, 075006, doi:10.1088/1748-9326/9/7/075006, 2014.

R Core Team: R: a language and environment for statistical computing, R Foundation for Statistical Computing, Vienna, Austria, available at: <http://www.R-project.org/> (last access: 24 July 2014), 2013.

Rawlins, M. A., Steele, M., Holland, M. M., Adam, J. C., Cherry, J. E., Francis, J. A., Groisman, P. Y., Hinzman, L. D., Huntington, T. G., Kane, D. L., Kimball, J. S., Kwok, R., Lam-

## Patterns and persistence of hydrologic carbon

B. W. Abbott et al.

[Title Page](#)

[Abstract](#)

[Introduction](#)

[Conclusions](#)

[References](#)

[Tables](#)

[Figures](#)



[Back](#)

[Close](#)

[Full Screen / Esc](#)

[Printer-friendly Version](#)

[Interactive Discussion](#)



mers, R. B., Lee, C. M., Lettenmaier, D. P., McDonald, K. C., Podest, E., Pundsack, J. W., Rudels, B., Serreze, M. C., Shiklomanov, A., Skagseth, Ø., Troy, T. J., Vörösmarty, C. J., Wenshanan, M., Wood, E. F., Woodgate, R., Yang, D., Zhang, K., and Zhang, T.: Analysis of the Arctic system for freshwater cycle intensification: observations and expectations, *J. Climate*, 23, 5715–5737, 2010.

Schuur, E. A. G., Vogel, J. G., Crummer, K. G., Lee, H., Sickman, J. O., and Osterkamp, T. E.: The effect of permafrost thaw on old carbon release and net carbon exchange from tundra, *Nature*, 459, 556–559, 2009.

Shirokova, L. S., Pokrovsky, O. S., Kirpotin, S. N., Desmukh, C., Pokrovsky, B. G., Audry, S., and Viers, J.: Biogeochemistry of organic carbon, CO<sub>2</sub>, CH<sub>4</sub>, and trace elements in thermokarst water bodies in discontinuous permafrost zones of Western Siberia, *Biogeochemistry*, 113, 573–593, 2013.

Slater, A. G. and Lawrence, D. M.: Diagnosing present and future permafrost from climate models, *J. Climate*, 26, 5608–5623, 2013.

Slavik, K., Peterson, B. J., Deegan, L. A., Bowden, W. B., Hershey, A. E., and Hobbie, J. E.: Long-term responses of the Kuparuk River ecosystem to phosphorus fertilization, *Ecology*, 85, 939–954, 2004.

Stottlemeyer, R.: Biogeochemistry of a Treeline Watershed, Northwestern Alaska, *J. Environ. Qual.*, 30, 1990–1998, 2001.

Striegl, R. G., Aiken, G. R., Dornblaser, M. M., Raymond, P. A., and Wickland, K. P.: A decrease in discharge-normalized DOC export by the Yukon River during summer through autumn, *Geophys. Res. Lett.*, 32, 1–4, 2005.

Striegl, R. G., Dornblaser, M. M., McDonald, C. P., Rover, J. R., and Stets, E. G.: Carbon dioxide and methane emissions from the Yukon River system, *Global Biogeochem. Cy.*, 26, GB0E05, doi:10.1029/2012GB004306, 2012.

Sullivan, P. F. and Sveinbjornsson, B.: Microtopographic control of treeline advance in Noatak National Preserve, Northwest Alaska, *Ecosystems*, 13, 275–285, 2010.

Tank, S. E., Frey, K. E., Striegl, R. G., Raymond, P. A., Holmes, R. M., McClelland, J. W., and Peterson, B. J.: Landscape-level controls on dissolved carbon flux from diverse catchments of the circumboreal, *Global Biogeochem. Cy.*, 26, 1–15, 2012.

Tarnocai, C., Canadell, J. G., Schuur, E. A. G., Kuhry, P., Mazhitova, G., and Zimov, S.: Soil organic carbon pools in the northern circumpolar permafrost region, *Global Biogeochem. Cy.*, 23, 1–11, 2009.



## Patterns and persistence of hydrologic carbon

B. W. Abbott et al.

Title Page

Abstract

Introduction

Conclusions

References

Tables

Figures



Back

Close

Full Screen / Esc

Printer-friendly Version

Interactive Discussion



Yurtsev, B. A., and Team, C.: The Circumpolar Arctic vegetation map, *J. Veg. Sci.*, 16, 267–282, 2005.

Walker, D. A., Reynolds, M. K., Maier, H. A., Barbour, E. M., and Neufeld, G. P.: Circumpolar geobotanical mapping: a web-based plant-to-planet approach for vegetation-change analysis in the Arctic, *Viten*, 1, 125–128, 2010.

Walter, K. M., Zimov, S. A., Chanton, J. P., Verbyla, D., and Chapin, F. S.: Methane bubbling from Siberian thaw lakes as a positive feedback to climate warming, *Nature*, 443, 71–75, 2006.

Wickland, K. P., Aiken, G. R., Butler, K., Dornblaser, M. M., Spencer, R. G. M., and Striegl, R. G.: Biodegradability of dissolved organic carbon in the Yukon River and its tributaries: seasonality and importance of inorganic nitrogen, *Global Biogeochem. Cy.*, 26, 1–14, 2012.

Wilhelm, E., Battino, R., and Wilcock, R. J.: Low-pressure solubility of gases in liquid water, *Chem. Rev.*, 77, 219–262, 1977.

Wlostowski, A. N., Gooseff, M. N., and Wagener, T.: Influence of constant rate versus slug injection experiment type on parameter identifiability in a 1-D transient storage model for stream solute transport, *Water Resour. Res.*, 49, 1184–1188, 2013.

WRCC: Western Regional Climate Center, available at: <http://www.wrcc.dri.edu/index.html> (last access: 19 June 2014), 2011.

Yoshikawa, K., Bolton, W. R., Romanovsky, V. E., Fukuda, M., and Hinzman, L. D.: Impacts of wildfire on the permafrost in the boreal forests of Interior Alaska, *J. Geophys. Res.-Atmos.*, 108, 1–14, 2002.

Zhang, T., Heginbottom, J. A., Barry, R. G., and Brown, J.: Further statistics on the distribution of permafrost and ground ice in the Northern Hemisphere, *Polar Geography*, 24, 126–131, 2000.

## Patterns and persistence of hydrologic carbon

B. W. Abbott et al.

[Title Page](#)

[Abstract](#)

[Introduction](#)

[Conclusions](#)

[References](#)

[Tables](#)

[Figures](#)



[Back](#)

[Close](#)

[Full Screen / Esc](#)

[Printer-friendly Version](#)

[Interactive Discussion](#)



**Table 1.** Characteristics of upland thermokarst features in study.

|  | Active layer detachment slide | Thermo-erosion gully | Retrogressive thaw slump |
|--|-------------------------------|----------------------|--------------------------|
| Outflow discharge ( $\text{L s}^{-1}$ )  | 2.8 (1.1)                     | 1.4 (0.4)            | 0.95 (0.3)               |
| Percent of outflow from ground ice       | 8.6 (5.5)                     | 37 (32)              | 49 (7.6)                 |
| $n^a$                                    | 7                             | 3                    | 16                       |
| Percent of features                      |                               |                      |                          |
| intersecting river/stream/water track    | 92                            | 56                   | 40                       |
| flowing into lake                        | 0                             | 38                   | 58                       |
| unassociated with water body             | 8                             | 6                    | 2                        |
| Percent of features occurring on         |                               |                      |                          |
| moist acidic tundra                      | 13                            | 53                   | 22                       |
| moist non-acidic tundra                  | 64                            | 5                    | 45                       |
| shrub tundra                             | 23                            | 42                   | 33                       |
| Percent of features in development stage |                               |                      |                          |
| 1  | 28                            | 32                   | 57                       |
| 2  | 36                            | 42                   | 17                       |
| 3  | 36                            | 26                   | 26                       |
| $n^b$                                    | 22                            | 34                   | 27                       |

Mean (SE) characteristics of upland thermokarst on the North Slope of Alaska. <sup>a</sup> Sample size for discharge and ground ice contribution measurements, <sup>b</sup> sample size for landscape position and development stage. Development stages were defined as follows: (0) no apparent present or past thermo-degradation, (1) active thermo-degradation (> 25 % of headwall is actively expanding) with completely turbid outflow, (2) moderate thermo-degradation (< 25 % of headwall is expanding) with somewhat turbid outflow, (3) stabilized or limited thermo-degradation with complete or partial revegetation and clear outflow.

## Patterns and persistence of hydrologic carbon

B. W. Abbott et al.

**Table 2.** Correlations between water chemistry parameters for 83 thermokarst features and 61 reference water tracks and first order streams.

|                                     | Activity     | DOC          | DON          | DOC: DON     | CO <sub>2</sub> | CH <sub>4</sub> | DIC         | NH <sub>4</sub> <sup>+</sup> | NO <sub>3</sub> <sup>-</sup> | N <sub>2</sub> O | SO <sub>4</sub> <sup>2-</sup> | Ca <sup>2+</sup> | Mg <sup>2+</sup> | K <sup>+</sup> | Na <sup>+</sup> |  |
|-------------------------------------|--------------|--------------|--------------|--------------|-----------------|-----------------|-------------|------------------------------|------------------------------|------------------|-------------------------------|------------------|------------------|----------------|-----------------|--|
| ln(DOC)                             | <b>0.34</b>  |              |              |              |                 |                 |             |                              |                              |                  |                               |                  |                  |                |                 |  |
| ln(DON)                             | <b>0.45</b>  | <b>0.94</b>  |              |              |                 |                 |             |                              |                              |                  |                               |                  |                  |                |                 |  |
| ln(DOC: DON)                        | <b>-0.43</b> | <b>-0.15</b> | <b>-0.46</b> |              |                 |                 |             |                              |                              |                  |                               |                  |                  |                |                 |  |
| ln(CO <sub>2</sub> )                | -0.08        | <b>0.27</b>  | <b>0.23</b>  | 0.13         |                 |                 |             |                              |                              |                  |                               |                  |                  |                |                 |  |
| ln(CH <sub>4</sub> )                | -0.13        | <b>0.18</b>  | 0.09         | <b>0.25</b>  | <b>0.59</b>     |                 |             |                              |                              |                  |                               |                  |                  |                |                 |  |
| DIC <sup>0.5</sup>                  | <b>0.25</b>  | -0.10        | 0.03         | <b>-0.35</b> | <b>-0.22</b>    | <b>-0.43</b>    |             |                              |                              |                  |                               |                  |                  |                |                 |  |
| NH <sub>4</sub> <sup>+(0.25)</sup>  | <b>0.52</b>  | <b>0.57</b>  | <b>0.59</b>  | <b>-0.30</b> | <b>0.16</b>     | 0.05            | 0.08        |                              |                              |                  |                               |                  |                  |                |                 |  |
| NO <sub>3</sub> <sup>- (0.25)</sup> | <b>0.42</b>  | <b>0.16</b>  | <b>0.24</b>  | <b>-0.24</b> | -0.14           | -0.07           | 0.00        | <b>0.38</b>                  |                              |                  |                               |                  |                  |                |                 |  |
| N <sub>2</sub> O <sup>(0.25)</sup>  | 0.12         | <b>0.38</b>  | <b>0.38</b>  | -0.06        | 0.14            | -0.02           | 0.03        | <b>0.42</b>                  | <b>0.39</b>                  |                  |                               |                  |                  |                |                 |  |
| SO <sub>4</sub> <sup>2-(0.25)</sup> | <b>0.40</b>  | 0.12         | <b>0.26</b>  | <b>-0.44</b> | <b>-0.31</b>    | <b>-0.41</b>    | <b>0.52</b> | <b>0.23</b>                  | <b>0.34</b>                  | <b>0.24</b>      |                               |                  |                  |                |                 |  |
| ln(Ca <sup>2+</sup> )               | <b>0.43</b>  | 0.07         | <b>0.25</b>  | <b>-0.52</b> | <b>-0.24</b>    | <b>-0.39</b>    | <b>0.67</b> | <b>0.18</b>                  | <b>0.34</b>                  | <b>0.20</b>      | <b>0.79</b>                   |                  |                  |                |                 |  |
| Mg <sup>2+(0.5)</sup>               | <b>0.43</b>  | 0.13         | <b>0.27</b>  | <b>-0.45</b> | <b>-0.27</b>    | <b>-0.45</b>    | <b>0.70</b> | <b>0.27</b>                  | <b>0.24</b>                  | 0.15             | <b>0.83</b>                   | <b>0.84</b>      |                  |                |                 |  |
| K <sup>+(0.25)</sup>                | <b>0.42</b>  | <b>0.30</b>  | <b>0.39</b>  | <b>-0.35</b> | <b>-0.22</b>    | <b>-0.23</b>    | <b>0.15</b> | <b>0.42</b>                  | <b>0.32</b>                  | <b>0.21</b>      | <b>0.48</b>                   | <b>0.39</b>      | <b>0.34</b>      |                |                 |  |
| ln(Na <sup>+</sup> )                | <b>0.47</b>  | 0.02         | <b>0.18</b>  | <b>-0.45</b> | <b>-0.37</b>    | <b>-0.50</b>    | <b>0.57</b> | <b>0.15</b>                  | <b>0.29</b>                  | 0.07             | <b>0.72</b>                   | <b>0.69</b>      | <b>0.73</b>      | <b>0.48</b>    |                 |  |
| ln(Cl <sup>-</sup> )                | <b>0.43</b>  | <b>0.43</b>  | <b>0.54</b>  | <b>-0.41</b> | <b>-0.20</b>    | <b>-0.25</b>    | <b>0.21</b> | <b>0.47</b>                  | <b>0.43</b>                  | <b>0.27</b>      | <b>0.48</b>                   | <b>0.37</b>      | <b>0.35</b>      | <b>0.63</b>    | <b>0.42</b>     |  |

Strength of relationships was determined by Pearson product-moment correlation. Significant correlations ( $p < 0.05$ ) are in bold. Relationships were visually inspected and transformed when necessary to meet the assumption of linearity (log and exponential transformations noted in the variable column on the left). All units are  $\mu\text{M}$  except dissolved gases (CO<sub>2</sub>, CH<sub>4</sub>, and N<sub>2</sub>O), which are ppmv, DOC: DON, which is a unitless ratio, and activity, which is recoded development stage 1–4 (low to high) treated as a non-parametric continuous variable.

Title Page

Abstract

Introduction

Conclusions

References

Tables

Figures

◀

▶

◀

▶

Back

Close

Full Screen / Esc

Printer-friendly Version

Interactive Discussion



## Patterns and persistence of hydrologic carbon

B. W. Abbott et al.

Title Page

Abstract

Introduction

Conclusions

References

Tables

Figures

◀

▶

◀

▶

Back

Close

Full Screen / Esc

Printer-friendly Version

Interactive Discussion



**Table 3.** Water chemistry for ground ice, thermokarst outflows and reference waters.

| Solute ( $\mu\text{M}$ )* | Ground ice   | Feature outflow | Reference water |
|---------------------------|--------------|-----------------|-----------------|
| DOC                       | 1213 (413)   | 2109 (349)      | 821 (120)       |
| DOC : DON                 | 18.7 (2.0)   | 27.1 (2.1)      | 33.8 (2.0)      |
| DIC                       | 953 (156)    | 893 (98)        | 587 (156)       |
| $\text{NH}_4^+$           | 54.7 (11.2)  | 42.5 (8.9)      | 2.08 (0.65)     |
| $\text{NO}_3^-$           | 2.68 (1.16)  | 3.95 (0.92)     | 1.96 (0.8)      |
| $\text{SO}_4^{2-}$        | 329 (101)    | 1042 (295)      | 76.9 (30)       |
| $\text{Mg}^{2+}$          | 416 (104)    | 854 (162)       | 219 (75)        |
| $\text{Ca}^{2+}$          | 441 (64)     | 894 (234)       | 173 (37)        |
| $\text{K}^+$              | 33.6 (5.4)   | 25.9 (4.5)      | 3.55 (1.1)      |
| $\text{Na}^+$             | 238 (42.1)   | 890 (303)       | 71.7 (23)       |
| $\text{Cl}^-$             | 137 (57.9)   | 1231 (561)      | 11.8 (3.9)      |
| $\delta^{18}\text{O}$     | -24.4 (0.92) | -21.6 (0.69)    | -19.2 (0.49)    |

Mean (SE) water chemistry from ground ice, outflow, and reference water for the 5 slides, 3 gullies, and 16 slumps where we sampled ground ice exposed by thermokarst formation. \* DOC : DON is a unitless ratio and  $\delta^{18}\text{O}$  is ‰.

## BGD

12, 2063–2100, 2015

## Patterns and persistence of hydrologic carbon

B. W. Abbott et al.

Title Page

Abstract

Introduction

Conclusions

References

Tables

Figures



Back

Close

Full Screen / Esc

Printer-friendly Version

Interactive Discussion

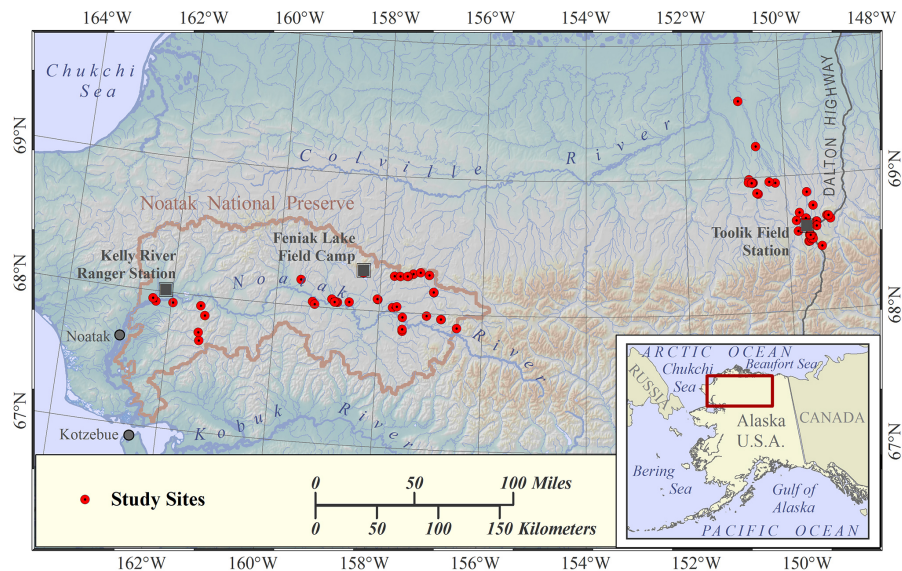


**Figure 1.** Map of study area. Features near the Kelly River Ranger Station were sampled in July of 2010, near Feniak Lake field camp in July of 2011, and near the Toolik Field Station in the summers of 2009–2012.

## Patterns and persistence of hydrologic carbon

B. W. Abbott et al.

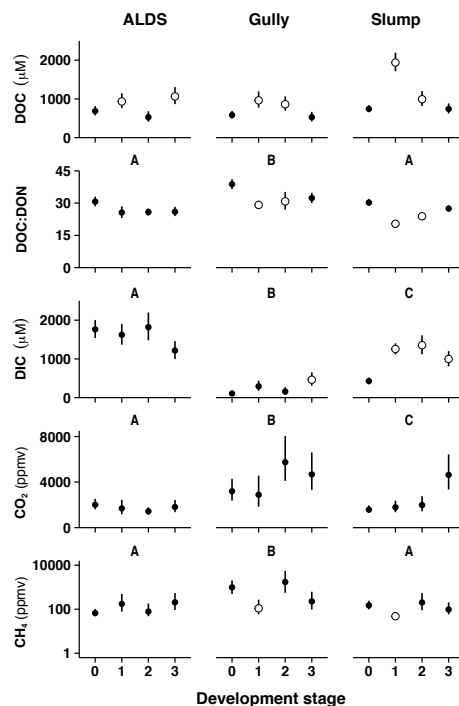


**Figure 2.** Dissolved carbon species and characteristics in outflow from 22 active-layer detachment slides, 19 thermo-erosion gullies, 42 thaw slumps, and 61 reference features in upland tundra on the North Slope of Alaska. Open circles signify statistical difference from stage-0 undisturbed sites,  $\alpha = 0.05$ . Different letters above panels represent significant differences between feature types. Error bars represent SE estimated by mixed-effects ANOVA after accounting for between-site variability. See Table 1 for complete definition of development stages: 0 = reference, 1 = most active, and 3 = stabilized. Note the log scale for  $\text{CH}_4$ .

Title Page

Abstract

Introduction

Conclusions

References

Tables

Figures



Back

Close

Full Screen / Esc

Printer-friendly Version

Interactive Discussion



## Patterns and persistence of hydrologic carbon

B. W. Abbott et al.

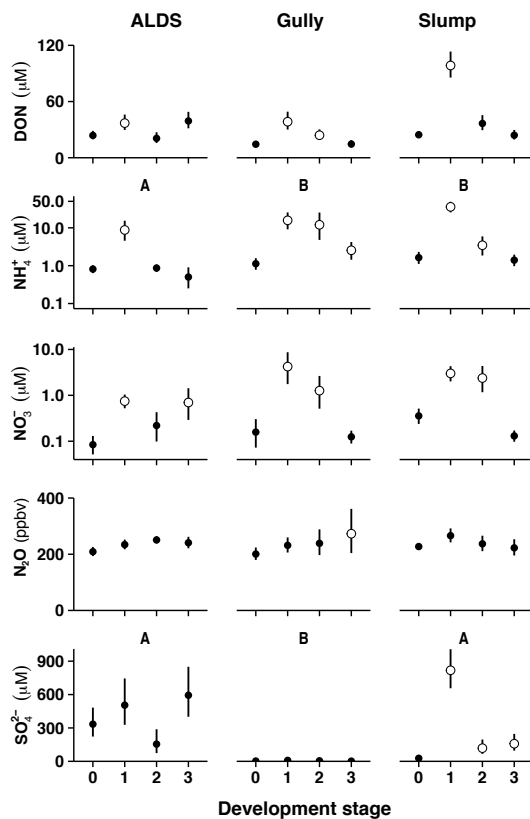


**Figure 3.** Nitrogen species and sulfate concentrations in outflow from 22 active-layer detachment slides, 19 thermo-erosion gullies, 42 thaw slumps, and 61 reference features. See Table 1 for complete definition of development stages: 0 = reference, 1 = most active, and 3 = stabilized. Note log scales for  $\text{NO}_3^-$  and  $\text{NH}_4^+$ . Symbology the same as Fig. 2.

Title Page

Abstract

Introduction

Conclusions

References

Tables

Figures



Back

Close

Full Screen / Esc

Printer-friendly Version

Interactive Discussion



## Patterns and persistence of hydrologic carbon

B. W. Abbott et al.

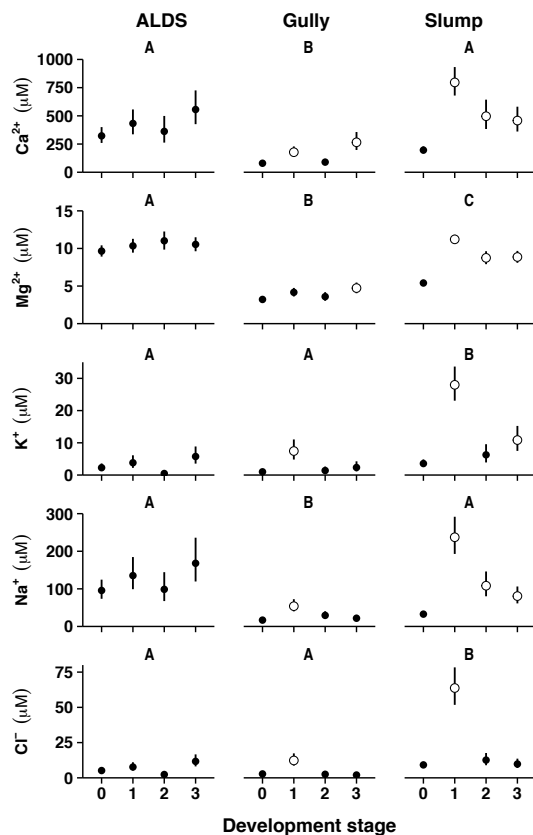


**Figure 4.** Major ion concentrations in outflow from 22 active-layer detachment slides, 19 thermo-erosion gullies, 42 thaw slumps, and 61 reference features. See Table 1 for complete definition of development stages: 0 = reference, 1 = most active, and 3 = stabilized. Note log scales for NO<sub>3</sub><sup>-</sup> and NH<sub>4</sub><sup>+</sup>. Symbology the same as Fig. 2.

Title Page

Abstract

Introduction

Conclusions

References

Tables

Figures



Back

Close

Full Screen / Esc

Printer-friendly Version

Interactive Discussion



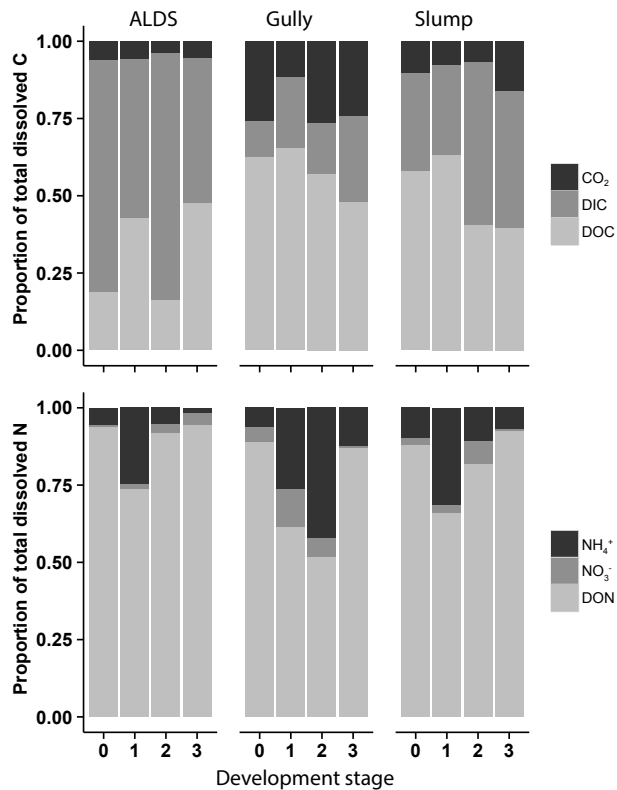


**Figure 5.** The relative proportion of carbon and nitrogen species in thermokarst outflow by feature type and development stage. See Figs. 2 and 3 for estimates of error and statistical tests for each parameter and Table 1 for complete definition of development stages: 0 = reference, 1 = most active, and 3 = stabilized.

Title Page

Abstract

Introduction

Conclusions

References

Tables

Figures



Back

Close

Full Screen / Esc

Printer-friendly Version

Interactive Discussion



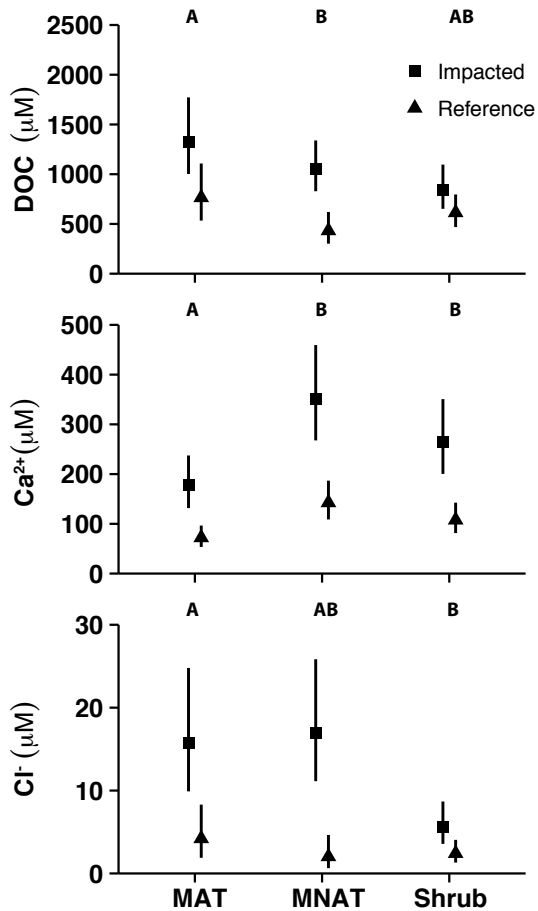


**Figure 6.** Mean ( $\pm 95\%$  CI) of parameters that varied significantly by surface age. Impacted and reference concentrations are shown independently when the interaction between thermokarst impact and surface age was significant, otherwise, results are combined.

## Patterns and persistence of hydrologic carbon

B. W. Abbott et al.

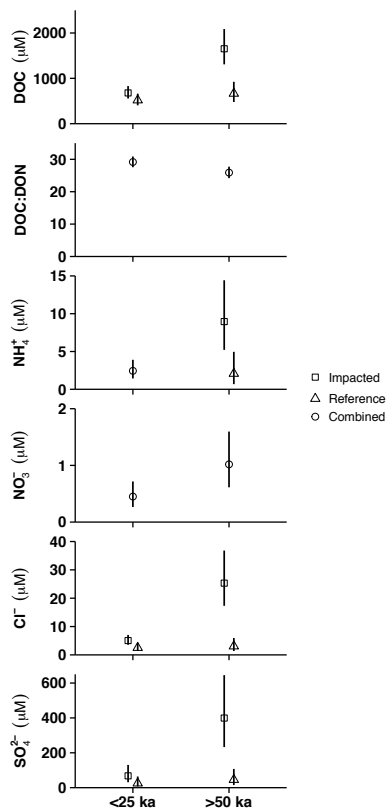


**Figure 7.** Mean ( $\pm 95\%$  CI) of DOC for thermokarst outflow and reference water from sites occurring on moist acidic (MAT), non-acidic (MNAT), and shrub tundra. Different letters above panels represent significant differences between feature types. DOC,  $\text{Ca}^{2+}$ , and  $\text{Cl}^-$  were the only parameters for which vegetation was a significant predictor in the mixed-effects ANOVA when accounting for development stage, feature type, and landscape age.